CALCULATING THE GEOMETRIC FACTOR IN A NEW EXPERIMENT ON RADIATIVE NEUTRON DECAY

Khafizov R.U.[a], Kolesnikov I.A.[a], Nikolenko M.V.[a], Tarnovitsky S.A.[a], Tolokonnikov S.V.[a], Torokhov V.D.[a], Trifonov G.M.[a], Solovei V.A.[a], Kolkhidashvili M.R.[a], Konorov I.V.[b]

[a]NRC «Kurchatov Institute», Russia
[b]Technical University of Munich, Munich, German

Abstract

This new experiment on radiative neutron decay will measure the branching ratio of radiative neutron decay. The methodology is focused on measuring the spectra of triple coincidences of radiative gamma-quantum, beta electron, and recoil proton together with the spectrum of double coincidences of beta electron and recoil proton. The peak on the spectrum of triple coincidences shows the number of radiative neutron decays, while the peak on the spectrum of double coincidences shows the number of regular neutron beta-decays. The ratio of these two numbers is proportional to the branching ratio, but the coefficient of the proportion (or its geometric factor) must be determined depending on the geometry of the equipment. This methodology enabled us to become the first team to measure the branching ratio of radiative neutron decay B.R. = $(3.2\pm1.6)10^{-3}$ (where C.L. = 99.7% and gamma quanta energy exceeds 35 keV) in 2005 on our old experimental equipment.

Now we have built new equipment to measure the branching ratio of radiative neutron decay, which we hope will allow us to measure with precision of several percentage points. This report is dedicated to conducting a computer simulation of the new experiment using the standard CERN program package Geant IV. One of the main goals of these Monte-Carlo calculations is to obtain the geometric factor and the background conditions for conducting the experiment. The report presents the results of these calculations. One of the main results of our computer experiment is the evaluation of background conditions, which shows that the geometry and materials we selected allow us to measure the branching ratio with precision of several percentage points.

PACS numbers: 13.30.Ce; 13.40.Hq; 14.20.Dh

Introduction

Among the many branches of elementary decay with charged particles in the final state, the radiative branch, where the decay occurs with the creation of an additional particle – the gamma quantum, is usually the most intensive, as the relative intensity (or branching ratio B.R.) of this mode is determined by the fine structure constant α of 10^{-2} order of magnitude. This decay branch is well established and was investigated for almost all elementary particles. However, the radiative decay of the free neutron

$$n \rightarrow p + e + \overline{\nu} + \gamma$$

was not discovered, and all the experiments were aimed at the study of the ordinary neutron decay branch.

However, the study of radiative branches of elementary particle decay occupies a central place in the fundamental problem of searching for deviations from the standard electroweak model. Characteristics of the ordinary decay mode are currently measured with

precision of tenths of a percentage point. Under these circumstances experimental data obtained by different groups of experimentalists can be reconciled only by taking into account the radiative corrections calculated within the framework of the standard theory of electroweak interactions. This means that experimental research of the ordinary mode of neutron decay has exhausted its usefulness for testing the standard model. To test the theory of electroweak interaction independently it is necessary to move from the research of the ordinary decay branch to the next step, namely, to the experimental research of the radiative decay branch.

The main value for radiative decay of neutron that is necessary to measure first of all is the relative intensity or branching ratio

$$BR = I(\text{radiative decay}) / I(\text{ordinary decay}) = N(e,p,\gamma) / N(e,p)/k = N_T / N_D/k$$

where the number of triple N_T and double N_D coincidences have to be taken directly from the experimental spectra of triple and double coincidences, thus the measurement of BR is really the measurement of the double e-p coincidences spectrum and the triple e-p-γ coincidences spectrum. Without analyzing these experimental spectra it is impossible to say anything about the experimental measurement of the BR value. The additional coefficient k is so called geometric factor what takes into account the geometry of experimental setup. The definition and calculation of k by using Monte Carlo simulation of the experiment with help of famous CERN program GEANT4 see "the calculation of geometric factor" part of this report.

For the neutron this rear branch of decay had not been discovered until recently and considered theoretically only [1–4]. Our first attempt to register the radiative neutron decay events was made on intensive cold neutron beam at ILL [5]. But our experiment conducted in 2005 at the FRMII reactor of Munich Technical University became the first experiment to observe this elementary process [6]. We initially identified the events of radiative neutron decay by the triple coincidence, when along with the two regular particles, beta electron and recoil proton, we registered an additional particle, the radiative gamma quantum and so could measure the relative intensity of the radiative branch of neutron decay B.R.= $(3.2\pm1.6)\cdot10^{-3}$ (with C.L.=99.7% and gamma quanta energy over 35 keV; before this experiment we had measured only the upper limit on B.R. at ILL [6]). A year after our discovery of the radiative neutron decay, a NIST experimental group published the results of their experiment on the study of the radiative neutron decay [7] in Nature, with their own value of B.R.= $(3.13\pm0.34)\cdot10^{-3}$ with C.L.=68% and gamma quanta energy from 15 to 340 keV. However, this group used strong magnetic field (see [7], and their recent article [8]) where the fast photomultiplier tube does not work and they should work with slow avalanche diodes. So, they got rough time resolution for their spectra. On other hand, in our last experiment we observe once more important phenomena – creation of ions with radiation of gamma-quanta. This effect can totally simulate the radiative decay of neutron if you have rough time resolution. So, the NIST team observes effect of the ion creation with the radiation of gamma-quanta. We conducted the detail comparison of our and NIST experiments in [9, 10] and this report presents Monte Carlo calculation of the geometric factor.

Theory

Our group carried out calculations of the neutron radiative spectrum in the framework of standard electroweak theory about twenty years ago [1–4]. After 10 years in the mid-2000 's work has been released [11], fully confirming our calculations. The calculated branching ratio

for this decay mode as a function of the gamma energy threshold is shown in Fig. 1. The branching ratio for the energy region investigated here, i.e. over 35 keV, was calculated to be about $2 \cdot 10^{-3}$ (gamma energy threshold ω on Fig. 1 is equal to 35 keV [3]).

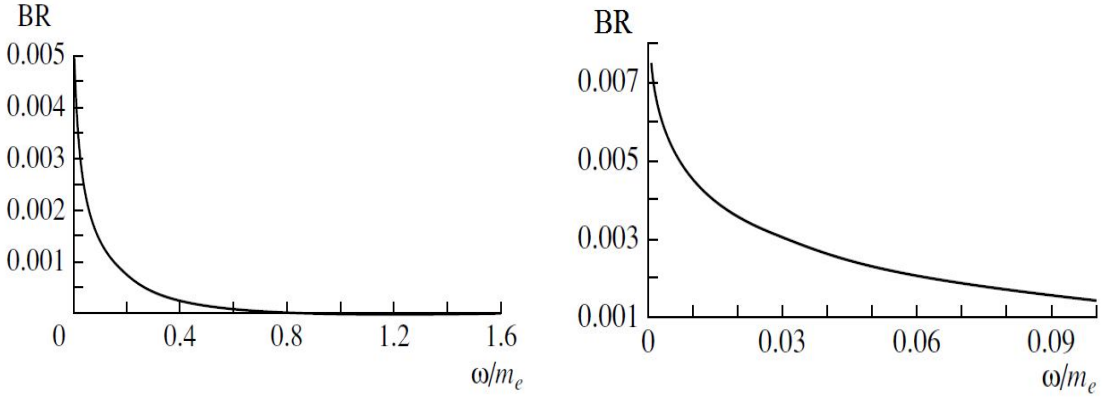

Fig. 1. The expected standard model branching ratio for radiative neutron beta decay (summed over all gamma energies larger than the threshold gamma energy ω) as a function of ω (from [1–4]).The left curve represents all values of ω and the right curve represents the low energy part of the spectrum.

Given this rather large branching ratio of about two per thousand, it is in principle not a difficult task to measure it. In practice, however, a rather significant background, mainly caused by external bremsstrahlung emitted by the decay electrons when stopped in the electron detector, has to be overcome. In this experiment this was achieved with the help of a triple coincidence requirement between the electron, the gamma-quantum and the recoil proton. The presence of such a coincidence is used to identify a radiative neutron decay event, whereas an ordinary neutron beta decay is defined by the coincidence of an electron with a recoil proton. The latter coincidence scheme is routinely used to measure the emission asymmetry of electrons in the decay of polarized neutrons [12-13]. Besides the non-correlated background one also has to deal with a correlated background of bremstrahlung gamma-quanta that fully simulates the desired fundamental radiative decay process searched for.

This correlated background is caused by bremsstrahlung emission of the electron traveling through the electron detector and is quite significant even when the thickness of this detector is limited to only a few mm. It cannot be eliminated by requiring a triple coincidence of the electron, the photon and the proton. However, calculations [3] show that the radiative emission of a photon in neutron decay is not in the forward direction with respect to the electron emission direction, as in the case of bremsstrahlung, but reaches a maximum intensity at an angle of 35° (Fig. 2). It was this property of radiative neutron decay that led us to use the space solution and register gamma quanta and electrons by different detectors, located at an angle to each other. To achieve this, we constructed a segmented electron-gamma detector with a 35° angle between the sections for electron and gamma detection to reduce background.

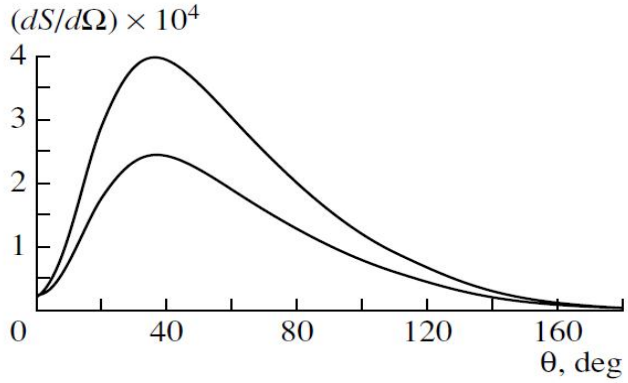

Fig. 2. Dependence of the radiative decay spectrum on the angle θ between the photon and the electron momenta (upper curve for a threshold gamma energy of 35 keV, lower curve for a threshold gamma energy of 50 keV) (from [3,4]).

Experimental setup

The experimental set-up is shown schematically in Fig. 3. The intense cold neutron beam passes through a rather long neutron guide in which is installed a collimation system made of LiF diaphragms, placed at regular distances of 1 meter. The neutrons enter the vacuum chamber (1) through the last diaphragm (9) that is located directly before the decay zone. This zone is observed by three types of detector: the micro channel plate (MCP) proton detector (3), the electron detector (13) consisting of a 7 cm diameter and 3 mm thick plastic scintillator, and six gamma detectors (11) that are located on a ring centered around the electron detector and which consist of photomultiplier tubes each covered with a layer of CsI(Tl) scintillator. The thickness of these 7 cm diameter CsI(Tl) scintillators is 4 mm and has been selected so as to have a 100% detection efficiency for photons. The six gamma detectors (11) surround the electron detector (13) (cf. the lower part of fig. 3) at an angle of 35° and are shielded from it by 6 mm of lead (12). By requiring a coincidence between the electron detector and any of the gamma detectors the bremsstrahlung background can in principle be overcome completely, because bremsstrahlung emission occurs only in the section that registers the electron. In this case, small part of the statistics is lost, of course, as can be seen from figure 2. However, the neutron beam intensity of 10^{12} n/s in our experimental chamber is sufficiently enough to compensate for that loss and still allows for a good count rate.

Recoil protons, formed in the decay zone, pass through a cylindrical time of flight electrode (7) in the direction of the proton detector (3) and are focused onto this detector with the help of spherical focusing electrodes (2). The focusing electrostatic field between the high voltage spherical and cylindrical electrodes (2) and (7) is created by the grids (5) and (6) at one side and by the proton detector grid (4), at ground potential, at the other side. It is important to note that the recoil protons take off isotropic from the decay point. In order not to lose the protons emitted towards the electron detector, an additional grid (10) is added on the other side of the decay volume.

The start signal that opens the time windows for all detectors is the signal from the electron, registered in the electron detector (13). For an event to be considered as a radiative neutron decay event there have to be simultaneous signals from the electron detector (13) and one of the gamma detectors (11), followed by a delayed signal from the proton detector (3). It is important to note that in the case of radiative decay, the gamma quantum in our equipment

is registered by gamma detectors (11) surrounding the electron detector (13) before the electron is registered by the electron detector. In other words, electron is delayed in

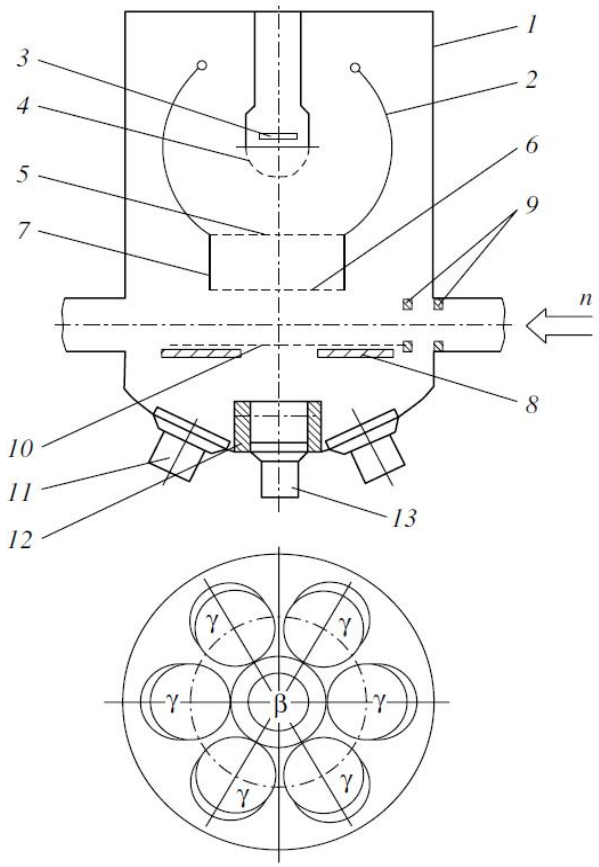

Fig. 3. Schematic lay-out of the experimental set-up: (1) detector vacuum chamber, (2) spherical electrodes to focus the recoil protons on the (at 18–20 kV), (3) proton detector, (4) grid for proton detector (at ground potential), (5) & (6) grids for time of flight electrode, (7) time of flight electrode (at 18–20 kV), (8) plastic collimator (5 mm thick, diameter 70 mm) for beta-electrons, (9) LiF diaphragms, (10) grid to turn the recoil proton backward (at 22–26 kV), (11) six photomultiplier tubes for the CsI(Tl) gamma detectors, (12) lead cup, (13) photomultiplier tube for the plastic scintillator electron detector.

comparison to the radiative gamma quantum. In the future namely this fact will allow us to distinguish the peak of radiative gamma quanta in the triple coincidences spectrum. Besides these triple coincidences also double electron-proton coincidences, signaling an ordinary neutron decay event, are monitored. It is important to note here that the installation of the LiF ceramics diaphragm (9) system in the neutron beam line has significantly reduced the gamma background from the intense cold neutron beam. The background level in the gamma detector amounted to about 2.5 kHz only (at a neutron beam intensity of 10^{10} n/s). If the number of the diaphragms in the neutron guide were doubled, the background of the gamma detectors could be further reduced by another order of magnitude, thus becoming comparable to the noise of the photomultiplier tubes. In the next section we present the results of our computer experiment where we used the geometry schematically demonstrated on Fig. 3. And we compare the loads of electron and gamma detectors with ones of our last experiment.

The geometric factor in computer experiment

All experiments are divided into two broad classes: absolute and relative. The absolute experiments measure a specific physical quantity that has a specific dimension. The relative experiments measure a dimensionless value and so avoid experimental uncertainties and from this point of view, they are easier to deliver. The value we seek to measure in our experiment is the ratio of N_T, the triple coincidences number of three radiative decay branch products - electron, recoil proton, gamma quantum to N_D, the double coincidences of standard beta-decay products – electron and recoil proton. This ratio is expressed in the relative intensity BR and a whole range of values, the so-called experimental uncertainties, which are quite difficult to determine in the experiment directly. Foremost of these uncertain valuesare the solid angles Ω_i for electron, gamma-quantum and recoil proton, as well as the registration efficiency ε_i for detectors of these particles:

$$\frac{N_T}{N_D} = \frac{\Omega_e \Omega_\gamma \Omega_p \varepsilon_\gamma \varepsilon_e \varepsilon_p}{\Omega_e \Omega_p \varepsilon_e \varepsilon_p} BR$$

As can be seen from the formula above, most of these uncertainties are cancelled out and the remaining ones define the geometric coefficient:

$$k = \Omega_\gamma \varepsilon_\gamma \qquad BR = \frac{1}{k}\frac{N_T}{N_D}$$

The formulas above work in the case when all three particles isotropically and independently fly in any direction, but as can be seen from Fig. 2 our experiment showed a strong correlation between the directions of the electron and gamma-quantum momenta. In other words, the radiative gamma-quantum is radiated anisotropically relative to an electron. In this case, the solid angle for an electron in the formula above Ω_e is not cancelled out and in computer experiment, the geometric coefficient k is calculated using the formula $k = N_{e\gamma}/N_e$, where $N_{e\gamma}$ is the number of paired electron-gamma coincidences where electron hits in the electronic detector (13) Fig. 3, and gamma quanta hits in one of 6 gamma detectors (11) Fig. 3. These events are generated inour computer experiment using GEANT4, the well-known CERN software package, using angular distribution for the angels between electron and gamma quantum directions shown on Fig. 2. N_e is simply the number of electrons registered in the electronic detector (13), theelectrons isotropic fly in any direction. Let us review these values in detail.

The results of Monte Carlo calculations are presented in Fig. 4–11. Fig. 4 shows the results of calculating Ne for a range of cases that vary the geometry of the intense cold neutron beam, namely its width w and the length l of its observable part. Fig. 4 shows various beam thickness h = 2, 3, and 4 cm while a beam width w, is held constant at 6 cm, while the volume density ρ of the generated beta-decay events per cubic centimeter equals to 5×10^5. Chart 4 clearly shows that the number N_e of electron hits grows in strict proportion to beam thickness h. This in turn means that N_e is dependent on the decay surface density per 1 cm^2 and is independent from beam thickness. Fig. 5 shows the values N_e for flat beams with widths of 8, 7, 6, 4 cm, while the surface density is one million decays per cm^2. Comparing curves obtained using flat beam 6 cm wide vs. using a beam of the same width but 2 cm thick shows that these curves coincide with accuracy of statistic fluctuations. This means that the volume of obtained statistics does not depend on the width of the beam, but rather depends only on the values of decays surface density, and this in turn means that the result of the experiment does not depend on the beam divergence. For all Figures the surface of the observable beam

part is equal to the square of a rectangle with sides of l and l/2 if $l<w$ and the square of a rectangle with sides w and l if $l>w$.

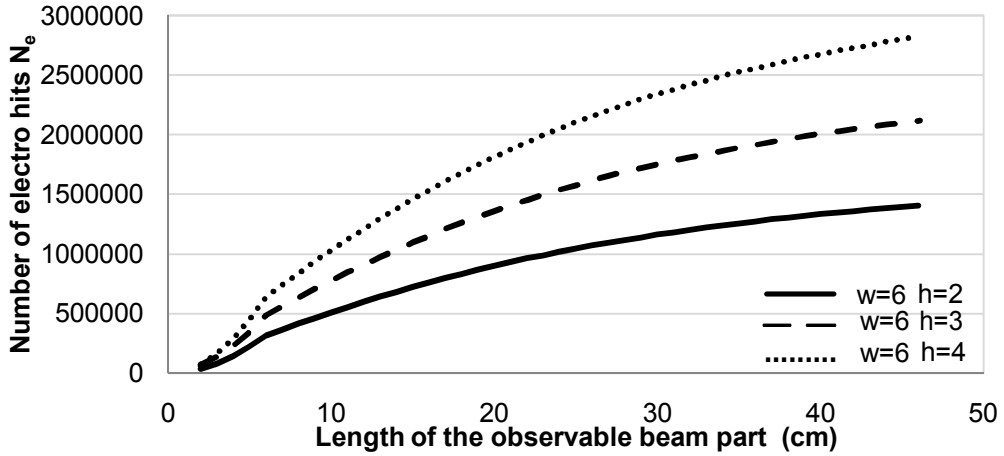

Fig. 4. Dependence of the electron hits N_e on the length l of the observable beam part for neutron beam with thickness h=2, 3, 4 cm and width w=6 cm. The number of the generated events is equal to 5×10^5 per 1cm^3.

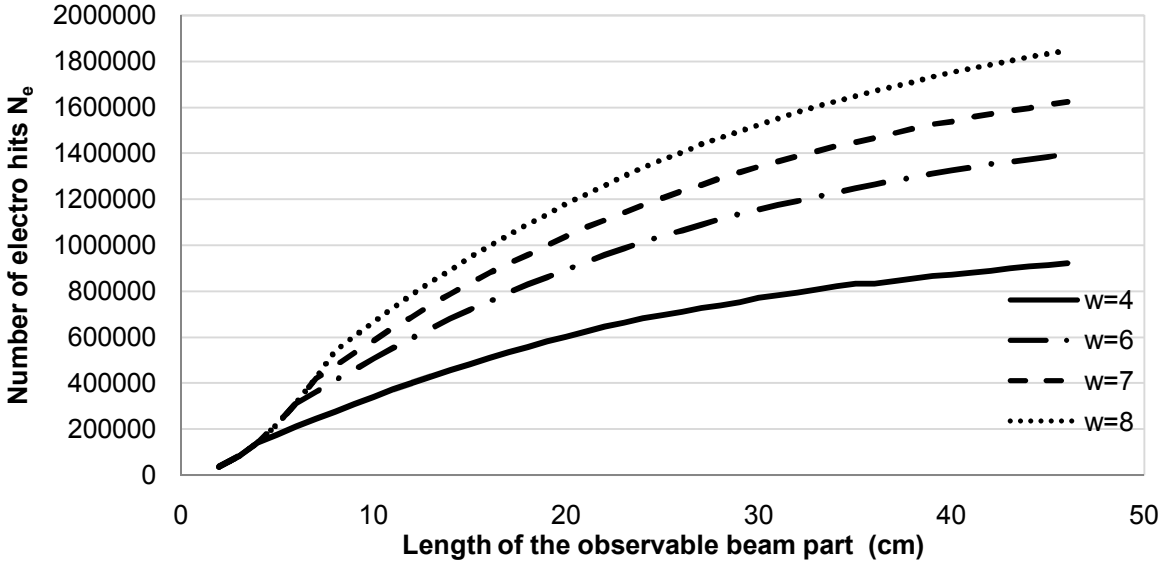

Fig. 5. Dependence of the electron hits N_e on the length l of the observable beam part for plane beam and various width w. Curves for plane beam with w=6 cm and for the beam with thickness h=2 cm on above Fig. 4 are in coincidence, so the result is not depend on divergence of neutron beam. The number of the generated events is equal to 10^6 per 1 cm^2.

Fig. 6 presents the geometric factor for electrons $k_e = N_e/N_{tot}$ where N_{tot}=ρhS is the total number of decays collected from the same beam surface as N_e. If electrons fly isotropically only from a central point, that lies at the intersection of the axis of the neutron beam and axis detector units (see Fig. 3), then $k_e = \Omega_e/(4\pi)$. Given that in our set-up the distance from the axis of the beam to the surface of electron detector is 142 mm, and the square electron detector with a diameter of 80 mm, we can calculate the value precisely at 0.018644, which coincides with the beginning of the curve in Figure 6 with accuracy of statistic fluctuations.

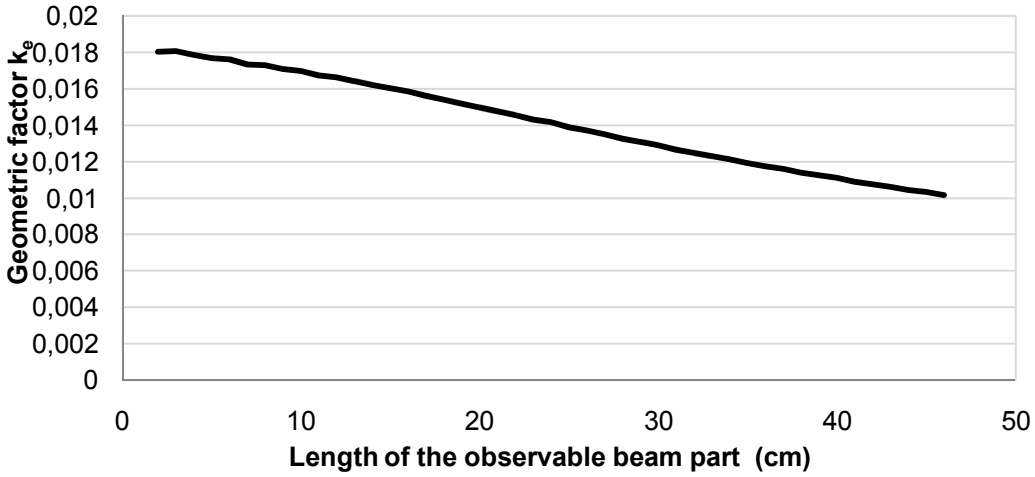

Fig. 6. Dependence of the electron factor k_e on the length l of the observable beam part. This value was within the same range for all cases.

We got similar graphs for the number of paired coincidences between an electron and gamma-quantum $N_{e\gamma}$. Graphs 7, 8, 9, 10 present the value of paired electron and gamma-quantum coincidences $N_{e\gamma}$, collected using the same beam width and thickness as the number of electron hits N_e. However, to arrive at the number of paired coincidences we conducted calculations in two cases, both for the isotropic case (shown on Figure. 7, 8), and anisotropic case on Fig. 8, 9, calculated using the angular distribution in Figure 2. The number of paired $N_{e\gamma}$ hits is certainly less relevant to values N_e, but the overall picture is similar: this value does not depend on the thickness of the beam, and the longer the observed part of the beam, the more smoothly it changes and almost goes to constant. This means that the result in this case does not depend on the divergence of the beam and the peripheral areas of the beam contribute less statistics the farther they get from the axis of detector units at Fig. 3.

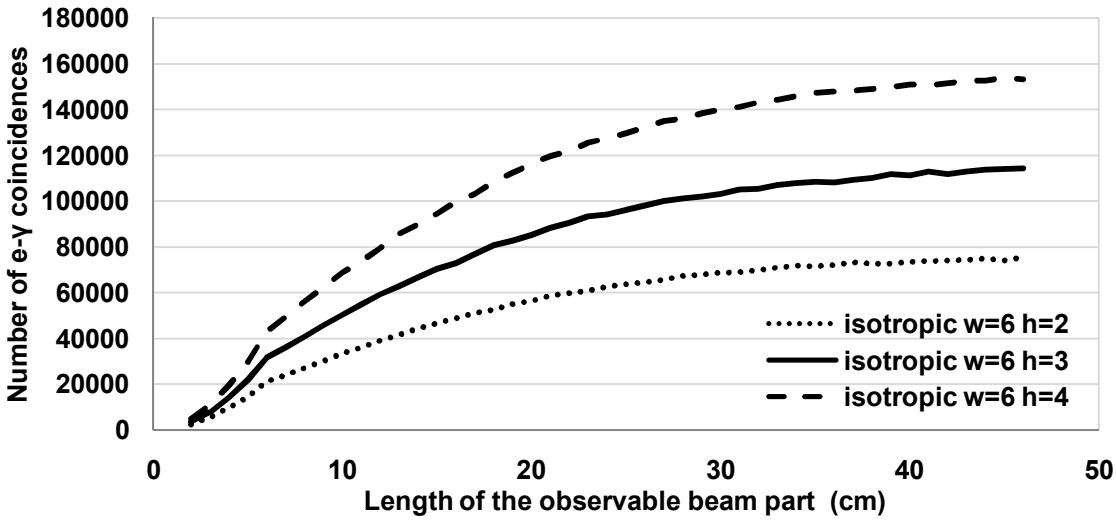

Fig.7. Dependence of e-gamma double hits on the length l of the observable beam part for isotropic case and beam with thickness h=2, 3, 4 cm and width w=6 cm. The volume density of the generated decays is equal to 5×10^5 events per 1 cm^3

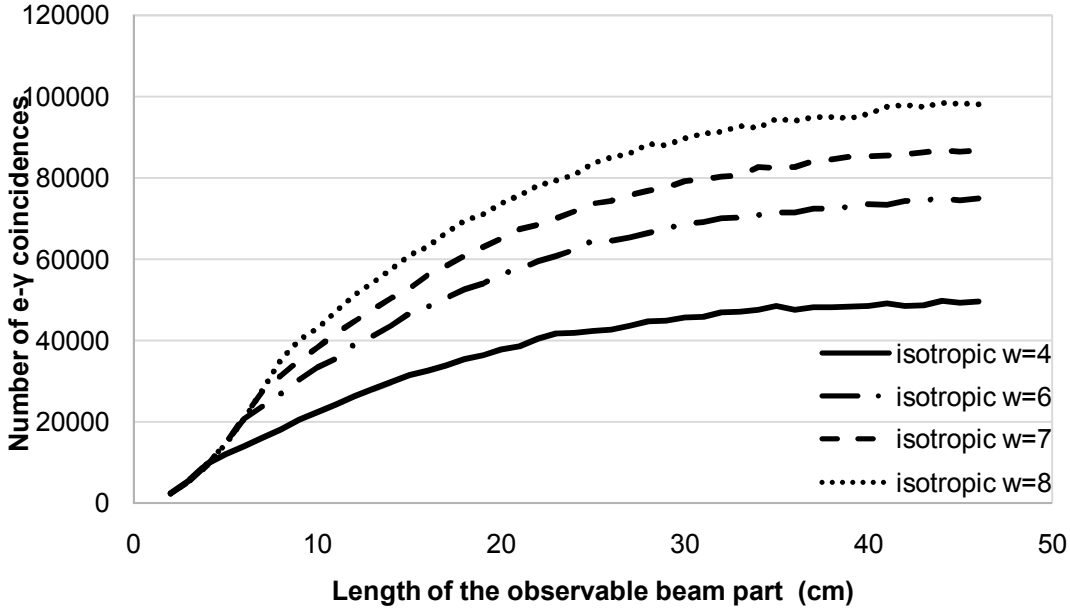

Fig. 8. Dependence of e-gamma double hits on the length *l* of the observable beam part for isotropic case and plane beam with width *w*=4, 6, 7, 8 cm. The surface density of the generated decays is equal to 10^6 events per 1cm^2. The plane beam with *w*=6 cm and the beam with the same width and thickness h= 2 cm (see Fig. 7) are in coincidence with accuracy of statistic fluctuations.

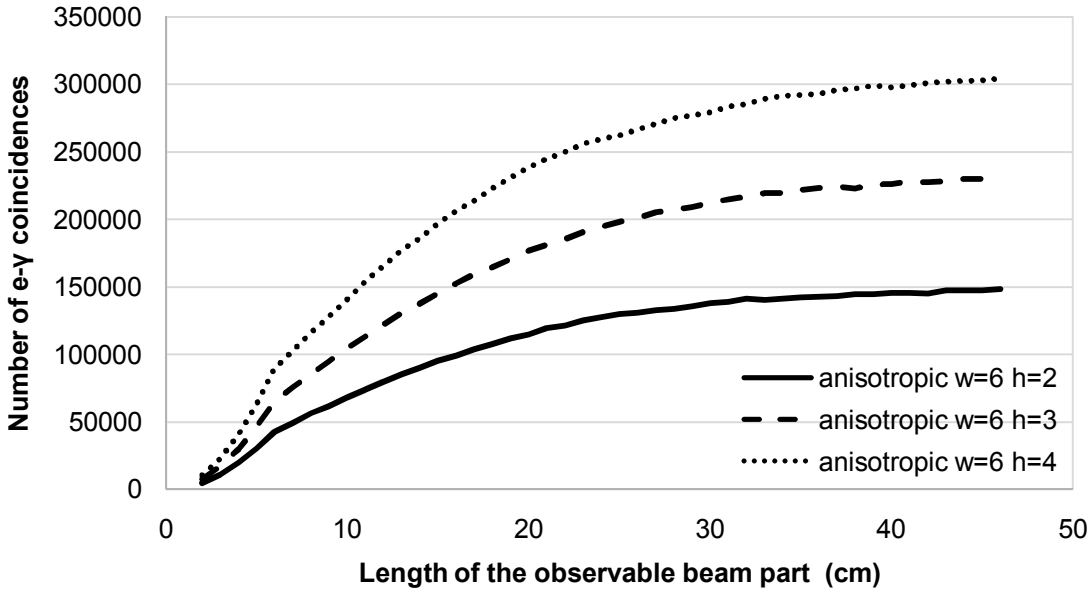

Fig. 9 is same as in Fig. 7 but for anisotropic case (see Fig. 2).

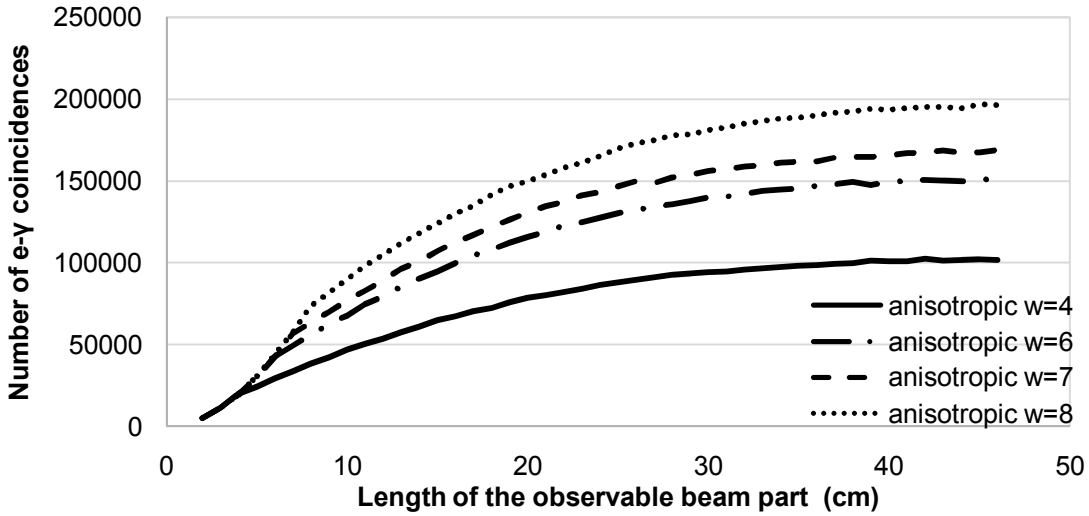

Fig. 10 is same as in Fig. 8 but for anisotropic case (see Fig. 2).

Finally, Fig. 11 presents the geometric factor $k = N_{e\gamma}/N_e$, required to calculate BR using the experimentally measured relationship N_T/N_D: BR = $N_T/N_D/k$. See isotropic and anisotropic cases on Fig. 11. It should be noted that curves for various beam widths and thicknesses coincide almost perfectly when it comes to the geometric factor. It should be noted that for a geometric factor curves for various beam widths and thicknesses with accuracy of statistic fluctuations. The comparison of both cases clearly demonstrates that the geometric factor of anisotropic case is double the size of the isotropic case. This, in turn, means, that we have correctly selected the geometry of the installation (see Figure 3), which best corresponds to the angular distribution in Fig. 2.

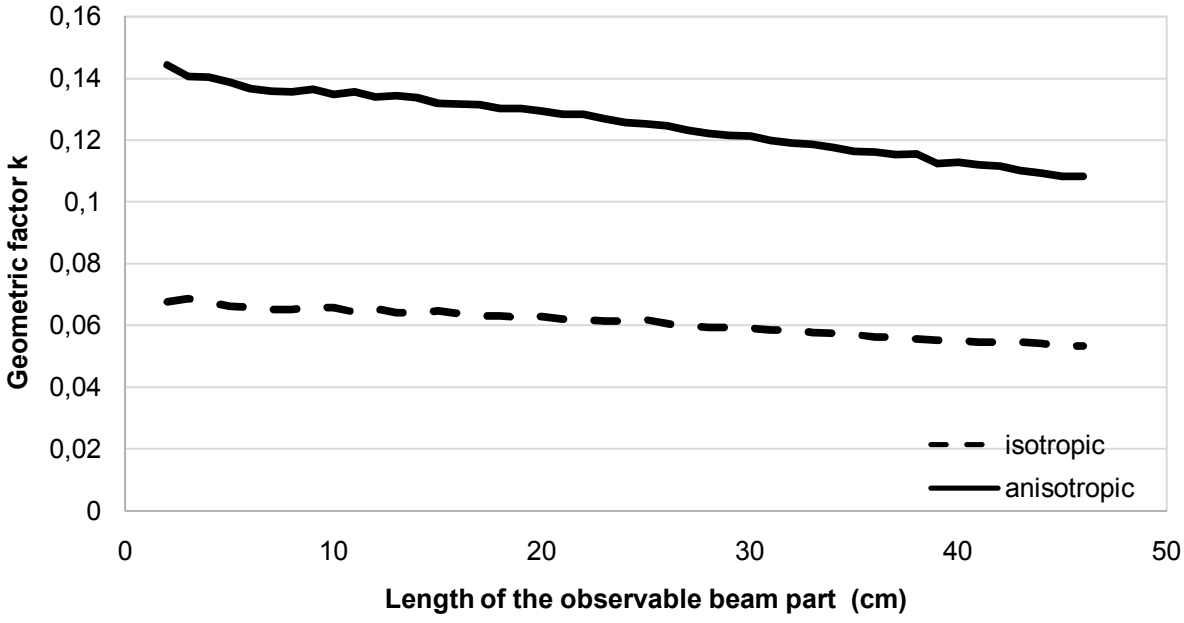

Fig. 11. Dependence of the geometric factor k necessary for the final BR determination on the length l of the observable beam part. This value is not sensitive to the beam width and thickness.

Let us now consider the intensity I_e of electron registration by electron detector on Fig. 3 and estimate the intensity of pair electron-gamma registrations by electron and 6 gamma detectors on Fig. 3. Let's define I_0 as the intensity of the cold neutron beams, neutron lifetime as τ_n, S_d– as square of lithium fluoride diaphragms, l - as the length of the observable part of the beam, and v_n– as the velocity of the cold neutrons. Then the intensity of the electronic registration by the electron detector can be expressed as:

$$I_e = I_0 S_d \frac{l}{v_n \tau} k_e = \frac{I_0 k_e}{v_n \tau_n} V = 2 \left(\frac{1}{cm^3 sec}\right) V$$

Here the coefficient in front of the observed beam volume V is calculated for the cold neutron beam intensity $I_0 = 10^{10}$ (n/cm^2 /sec), $v_n = 10^5$ (cm/sec), and k_e is taken at maximum on Fig. 6. Under these conditions, it is easy to appreciate that the density in 1 cm^3 we simulated in the computer experiment 5×10^5 decays can be collected in three days on the intensive neutron beam. This formula can be used to estimate the intensity of the electron registration, depending on the observed volume V. In our last experiment, this value was about 200 cm^3, so we estimate for the count rate of a few hundred electrons per second. This order of magnitude corresponds to the count rate that we observed in our last experiment, which was equal to 100 Hz. To estimate the intensity of electron-gamma coincidences, we need to multiply I_e by the value of the geometric factor k from Fig. 11, in the order of 10^{-1}, and BR value taken from Fig. 1, in the order of 10^{-3}. As a result, we estimate the count rate of the electron-gamma coincidences equal to one event per 100 seconds.

This rate of statistics collection is quite high, however, in our latest experiment the count rate of the triple coincidences was less in 1–2 orders of magnitude. This is due to the fact that the coincidence with protons depends not only on the geometry and electrode voltages on electrodes in Fig. 3, but also and primarily by the value of the ion background. The fact of the matter is that ions are formed in huge quantities in the presence of the intense cold neutron beam throughout the whole volume (about 1 m^3) of the entire experimental setup. The number of recoil protons is negligible in comparison to the number of ions, and even when the pressure in the chamber reached 10^{-4} mbar, the proton peak literally "downed" in the high ionic background and only at a pressure of 10^{-6}–10^{-7} mbar it came to stand out above the ion background and the height of the ion background horizontal substrate became equal to the height of the proton peak. Detailed consideration of the baseline conditions of the experiment and, above all, the phenomenon of ionization would be discussed separately in the next report.

The authors would like to thank Profs. D. Dubbers and Drs. T. Soldner, G. Petzoldt and S.Mironov for valuable remarks and discussions. We would especially like to thank RRC President Academician E.P. Velikhov and Prof. V.P. Martem'yanov for their support. Financial support for this work was obtained from RFBR (Project N 14-02-00174).

References

1. GaponovYu.V., Khafizov R.U. Phys. Lett. B **379** (1996) 7–12.
2. Radiative neutron beta-decay and experimental neutron anomaly problem. By Yu.V. Gaponov, R.U. Khafizov. Weak and electromagnetic interactions in nuclei (WEIN '95): proceedings. Edited by H. Ejiri, T. Kishimoto, T. Sato. River Edge, NJ, World Scientific, 1995, 745p.

3. R.U. Khafizov, N. Severijns. Proceedings of VIII International Seminar on Interaction of Neutrons with Nuclei (ISINN-8) Dubna, May 17–20, 2000 (E3-2000-192), 185–195.
4. Khafizov R.U. Physics of Particles and Nuclei, Letters **108** (2001) 45–53.
5. M. Beck, J. Byrne, R.U. Khafizov, et al., JETP Letters **76** (2002) 332.
6. R.U. Khafizov, N. Severijns, O. Zimmer et al. JETP Letters **83** (2006) 5.
7. J.S. Nico, et al. Nature, **444** (2006) 1059–1062.
8. M.J. Bales, R. Alarcon, C. D. Bass, et al., Phys. Rev. Lett. **116** (2016) 242501.
9. R.U. Khafizov, S.V. Tolokonnikov, V.A. Solovei and M.R. Kolhidashvilli. Russian Yad. Fiz. **72**(2009) 2102.
10. Khafizov R.U., Kolesnikov I.A., Nikolenko M.V. et al. Proc. of the XXIth International Seminar on Interaction of Neutrons with Nuclei; Neutron Spectroscopy, Nuclear Structure, Related Topics, Dubna, 2014, Reports, p. 114.
11. V. Bernard, S. Gardner,Ulf-G. Meißner and Chi Zhang. Phys. Lett. B **593** (2004) 105.
12. B. G. Yerozolimsky, Yu. A. Mostovoi, V P. Fedunin, et al., Yad. Fiz. **28** (1978) 98; [Sov. J. Nucl. Phys. **28** (1978)48].
13. I.A. Kuznetsov, A. P. Serebrov, I. V. Stepanenko, et al., Phys. Rev. Lett., **75** (1995) 794.